Sensitive electrochemical recognition of *α*-Synuclein protein in human plasma sample using bioconjugated gold nanoparticles: An innovative immuno-platform to assist in the early stage identification of Parkinson's disease

Esmaeil Darvish Aminabad [a,b], Mohammad Hasanzadeh [b,c*], Ali Ahmadalipour [d], Mohammad Ali Hosseinpour Feizi [a,**], Reza Safaralizadeh [a], Ahmad Mobed [d,f]

[a] Department of Biology, Faculty of Natural Sciences, Tabriz University, Tabriz, Iran

[b] Pharmaceutical Analysis Recent Center, Tabriz University of Medical Sciences, Tabriz, Iran

[c] Nutrition Research Center, Tabriz University of Medical Sciences, Iran.

[d] Research Center of Psychiatry and Behavioral Sciences, Tabriz University of Medical Sciences, Tabriz, Iran

[f] Aging Research Institute, Faculty of Medicine, Tabriz University of Medical Sciences, Iran

Corresponding author at:
*Pharmaceutical Analysis Recent Center, Tabriz University of Medical Sciences, Tabriz 51664, Iran.
Hasanzadehm@tbzmed.ac.ir
** Department of Biology, Faculty of Natural Sciences, Tabriz University, Tabriz, Iran
MH-Faizi@ea-sciencepark.org.ir

This article has been accepted for publication and undergone full peer review but has not been through the copyediting, typesetting, pagination and proofreading process which may lead to differences between this version and the Version of Record. Please cite this article as doi: 10.1002/jmr.2952

Abstract

This research work explains the development of an electrochemical immunosensor for the selective recognition of SNCA in human biofluids. An innovative protocol was proposed for the green synthesis of gold nanoparticle supported dimethylglyoxime (AuNPs@DMGO) using one step electrogeneration method. Also, application of AuNPs@DMGO for the sensitive quantification of α-Synuclein (SNCA) protein and its biomedical analysis. So, an innovative sandwich immunosensor was designed for the sensitive identification of SNCA antigen in aqueous solution. The gold nanoparticles (AuNPs) was decorated on the surface of glassy carbon electrode by chronoamperometry technique to provide appropriate immobilization surface with large number of active sites for immobilization of specific biotinylated antibody (Ab1) and against SNCA protein. Then, the sandwich-type immuno-platform was completed by the attachment of secondary antibody (HRP conjugated Ab (Ab2)) to the primary complexes on the surface of electrode. For the first time, α-Synuclein protein was measured with an acceptable linear range of 4 to 64 ng/ml and lower limit of quantification of 4 ng/ml. Benefiting from the simplicity and high sensitivity, the proposed method shows a potential of employment in clinical applications and high-throughput screening of Parkinson's disease using POC.

Keywords: α-Synuclien, Parkinson's disease, biorecognition, Immunosensor, Protein, biomedical analysis.

1. Introduction

Parkinson's disease as one of the most common progressive neurological disorders with several motor and non-motor symptoms, such as rigid muscles, tremor, slowed movement, speech and emotional changes, loss of automatic movements, writing changes and thinking difficulties has reduced life expectancy [1-3]. The progressive nervous system ailment results primarily from the disruption or death of dopaminergic neurons in the *substantia nigra* of the midbrain [4-6]. Subsequently, various of the symptoms are begin to observe owing to the destruction of neurons that produce dopamine as the most significant neurotransmitter [7]. Therefore, unusual brain activity and several symptoms are originated due to low concentrations of dopamine in human body [8]. Although surgical treatment and medications might significantly improve and recover patient symptoms and control certain regions of the brain, however its detection at early stages may improve the treatment. The stages of this disease can be determined by various important factors associated with Parkinson's disease including gens, environmental triggers, specific microscopic markers within brain cells, and α-synuclein found within lewy bodies [9, 10].

The α-synuclein, as a main natural protein in Parkinson's patients, has attracted considerable attention for detection of Alzheimer's disease [11, 12]. It has been frequently observed in human at the tips of neurons in particular structures recognized as presynaptic terminals [13]. Although the full physiological function of α-synuclein is yet to be determined and there may be contradictory findings about it but some approved functions of α-synuclein are neurotransmitter release and regulation of vesicle docking in synaptic activity [14]. Furthermore, the accumulation rout of α-synuclein is exhibited in Scheme 1 [15].

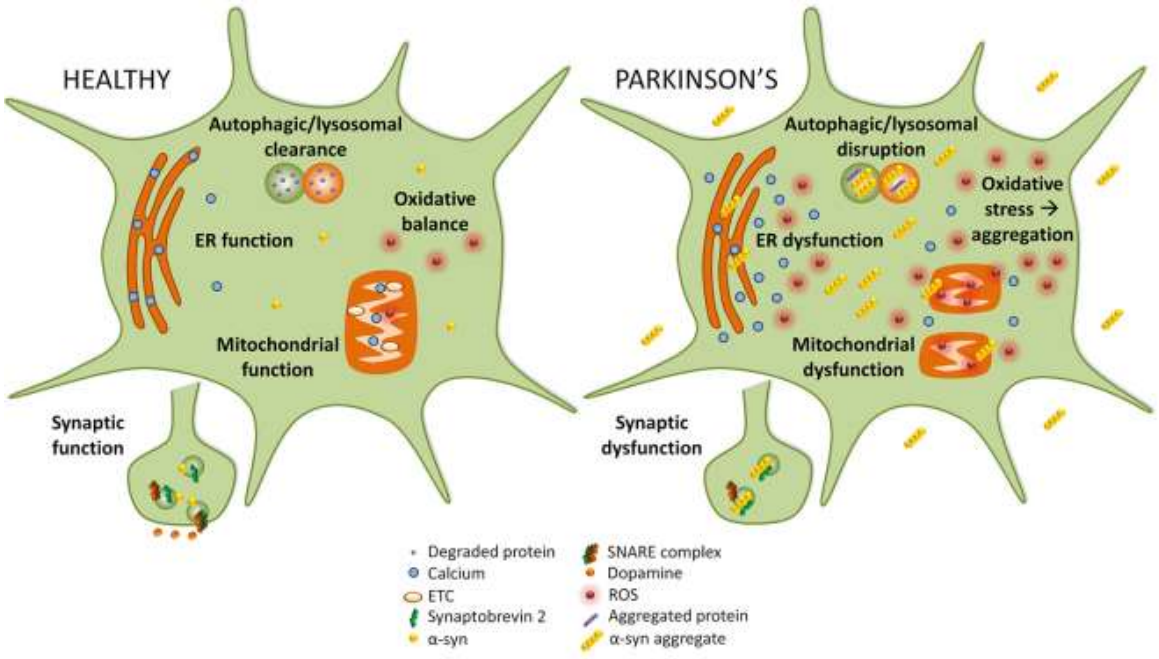

Scheme 1. The accumulation effect of α-synuclein [1]

This protein linked genetically and neuropathologically to Parkinson's disease and play significant role in Parkinson's disease pathogenesis due to mediate neuronal death and disturbance of cellular homeostasis and, through effects on several intracellular targets, as well as synaptic function [16, 17]. In addition, seeding of aggregation is one of the toxic effects of α-synuclein leakage to nearby cells. Thus, it conceivably contributes to Parkinson's disease propagation [18]. Therefore, this biomarker is of great value and importance for detection of Parkinson's disease. Over the last decades, several conventional methods such as enzyme-linked immunosorbent assay (ELISA) [19], polymerase chain reaction (PCR) [20] and real-time PCR [21] have been exploited for determination of α-synuclein protein or its genetic counterparts. Some drawbacks including time consuming procedure, high costly, low specificity and sensitivity have encouraged researchers to new techniques for its quantification in biological matrixes [22]. Thus, sensors as a novel, simple and rapid sensing tools have attracted great attention to overcome the

drawbacks of traditional techniques and provide several advantages such as simplicity, cost-effectiveness, as well as high sensitivity and specificity [23]. Over the last few years, different type of sensors have been developed for the detection of α-synuclein protein consisting of electrochemical [24], optical [25], and quartz crystal microbalance (QCM) [26]. Among different types of sensors, electrochemical based sensors benefits from several features such as being practical, sensitive, fast, selective, and having low detection limits [27]. Meanwhile, various types of bioreceptors such as antibodies, enzymes and nucleic acids as efficient factor for improving sensitivity and selectivity of have used on the electrochemical electrode [28], however, antibodies provide a reliable and suitable opportunity for biomarker detection as a bioreceptor, especially in electrochemical sensors [29]. On the other hand, with the development of nanoscience and nanotechnology, AuNPs have enabled significant improvement in the analytical performance of electrochemical sensors due to high surface area, high conductivity and ability to carry large number of functional groups [30-32].

In this study, we developed high specific and sensitive electrochemical immunosensor based on AuNPs for detection of α-synuclein protein. For this purpose, the surface of GCE was firstly modified with AuNPs to provide excellent substrate towards strong immobilization of biotinylated Ab (Ab1). The engineered electrode surface (GCE-AuNPs-Ab1) could successfully capture SNCA protein. At the end, secondary Ab2 (HRP-Ab) was conjugated with modified surface (GCE-AuNPs-Ab1-SNCA) to result sandwich type electrochemical immunosensor. Finally, this electrochemical sandwich based immunosensor could able to determine low concentrations of SNCA in human plasma samples.

2. Materials and methods

2.1. Chemicals and reagents

All chemicals used in this research were of analytical grade (purity of 99%). Potassium ferrocyanide $K_4Fe(CN)_6$, potassium ferricyanide $K_3Fe(CN)_6$, sodium acetate, hydrogen tetrachloroaurate(III)hydrate ($HAuCl_4 \cdot 3H_2O$) and bovine serum albumin (BSA) were all obtained from Sigma-Aldrich (Ontario, Canada). Furthermore, dimethylglyoxime, ethanol and sulfuric Acid (H_2SO_4) were purchased form Merck (Germany). A human α -synoclein kit containing biotinylated antibody, HRP-conjugated antibody and various concentrations of the antigen was purchased from ZellBio GmbH (Germany) by Padgin TEB Company. Piranha solution was prepared by mixing hydrogen peroxide and concentrated sulfuric acid in a 1:2 (v/v) ratio. A ferricyanide/ferrocyanide solution containing 0.5 M KCl and 0.5 M of $K_4Fe(CN)_6/K_3Fe(CN)_6$ (1:1) were prepared for the electrochemical assessment of the microscopic surface areas of the working electrodes. It was prepared immediately prior to use to maintain its reactivity. All the above solutions were kept at4 °C before use. Human plasma samples was prepared from Blood Transfusion Research Center (Tabriz, Iran). All of materials were used without further purification.

2.2. Apparatuses and methods

In this conceptual study, electrochemical measurements and electrodeposition were operated by using an ordinary three-electrode cell (from Metrohm) containing Ag/AgCl as a reference electrode, a platinum wire as an auxiliary electrode and a GCE (from Azar Electrode Co., Urmia, Iran) as a working electrode (d=2 mm). The experiments were run by an electrochemical AUTOLAB PGSTAT 302N system (Eco Chemie, Utrecht, The Netherlands). The system was powered on a PC using NOVA 1.1 software. FE-SEM (Hitachi-Su8020, Czech) with a working

voltage of 3 kV and EDX (model: MIRA3 TESCAN, Brno, Czech Republic) were exploited for morphological study and chemical compositions of the surface of electrode, respectively.

2.4. Fabrication of immunosensor

Briefly, 0.0464 g dimethylglyoxime was dispersed completely in 2 ml of ethanol. Then, 2 mL of hydrogen tetrachloroaurate (III) hydrate ($HAuCl_4 \cdot 3H_2O$) (30 mM) was added to it followed by the addition of11 µL 50 mM H_2SO_4 media. The synthesized nanoparticles dispersion was stored in dark place.

Prior to any modification, the physical and electrochemical cleaning of the electrode surface were performed to remove any probable contamination on electrode surface. For physical cleaning, electrode surface was polished with 0.05 µm alumina (Beuhler, USA) on a standard pad and then electrode was rinsed with a solution of deionized water to obtain a mirror-like surface. For electrochemical treatment, the potential of GCE was cycled 20 times between -0.2 to 0.8 V in 0.5 M H_2SO_4 by cyclic voltammetry (CV) technique. After cleaning, the electrode was dried at room temperature.

The GCE-AuNPs-Ab1-BSA-SNCA-Ab2 were prepared as following: initially, AuNPs was electrogenerated on the surface of GCE by ChA technique at the E=0 V and duration time of 500 s (Figure S1 (see supporting information)). Thus, the modification of GCE with AuNPs provided appropriate and excellent surface for immobilization of Ab1. Then, 50 µl of the biotinylated antibody solution was transferred to an autoclaved vial and then exposed to the 100 µl of EDC solution Then, GCE-AuNPs was decorated with activated Ab1 (10 µL) by drop casting technique at 4 ° C for 4 h. After incubation and complete drying, the electrode surface was washed with distilled water. Afterward, 10 µL of BSA, as blocking agent, was drop casted on the surface of GCE-AuNPs-Ab1 to block any remaining area and to reduce non-specific adsorption during 40

min. At the third stage, 10 µL antigen with 32 ng/ml concentration of SNCA was incubated at 4 ° C for 1 h on the surface of modified electrode (GCE-AuNPs-Ab1-BSA) for efficiently linkage to Ab1. At the end, the secondary Ab2 (HRP-Ab2) was drop casted on the surface of engineered surface (GCE-AuNPs-Ab1-BSA-SNCA) for 2 h at 4 °C (Scheme 2). Finally, the electrochemical properties of the sandwich-type immunosensor in comparison with other electrodes were evaluated by voltammetry and amperometry techniques.

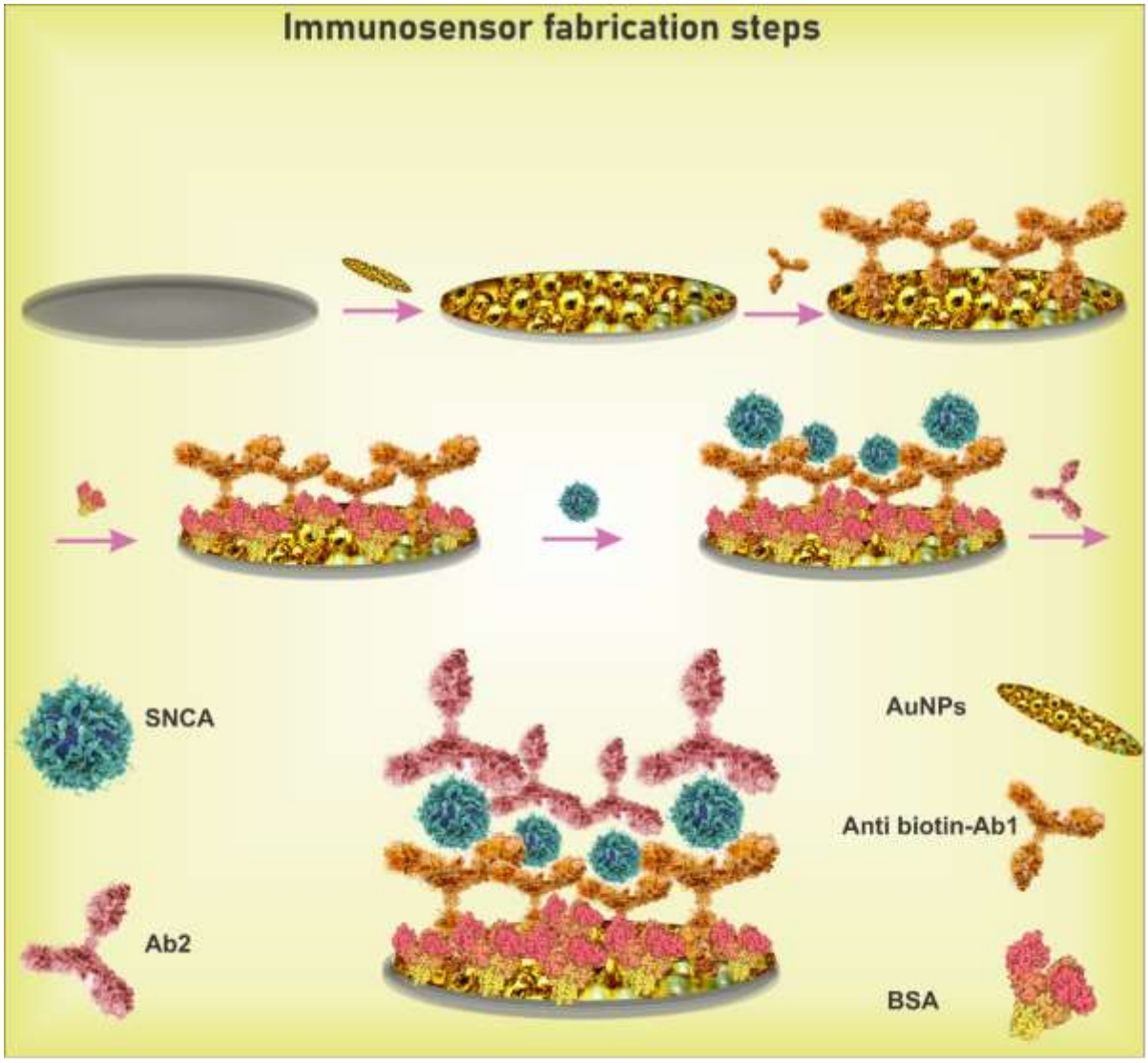

Scheme 2. Iilustration prepration sandwich type electrochemical immunosensor for the detection of SNCA.

3. Results and discussion

3.1 Characterization and stability assessment of AuNPs in the fabricated immunosensor

For morphology and structural evaluation of modified GCE with AuNPs, FE-SEM images and EDX have demonstrated in Figure S2 (A-K (see supporting information)). As seen, although the size of the synthesized nanoparticles on the electrode surface is between 40-100 nm, sizes of the most particles are between 45-60 nm. The modification of GCE surface with AuNPs demonstrated scattered topographies. Furthermore, roughness of the surface mostly enhanced with increasing nanoparticle-grafting density. In addition, the rate of changes was not the same in different regions of the electrode surface. The result of EDX analysis (Figure S2K (see supporting information)) exhibited of the presence of Au element due to modification of surface with electrodeposited nanoparticles. Therefore, the results of both tests proved that the AuNPs were successfully electrodeposited on the surface of GCE.

In the other to study the stability of nanoparticles on the electrode surface, the cyclic voltammograms of 0.01 M Ferrocyanide/Ferricyanide solution, as electrochemical probe, within 0.5 M KCl were recorded for intraday, inter-day and multiple cycling of GCE-AuNPs (Figure S3 (A-F (see supporting information)). In details, inter-day stability of AuNPs on the surface GCE was tested by carrying out CV technique 5 times (every 2 h) within a day at similar conditions and time intervals. According to obtained results (Figure S3 (A and D) (see supporting information), the performance of AuNPs remained almost constant. Furthermore, an investigation of the intraday test showed that the function of AuNPs on the surface of GCE was decreased only 44% after four days (Figure S3 (B and E) (see supporting information). As shown in Figure S3 (C and F) (see supporting information), the performance of GCE-AuNPs was not

reduced even after 100 cycles, representing considerable stability of designed electrode for biosensing applications.

3.2 Electrochemical behavior of developed immunosensor

All of the modification and detection steps of the electrode (GCE, GCE-AuNPs, GCE-AuNPs-Ab1, GCE-AuNPs-Ab1-BSA, GCE-AuNPs-Ab1-BSA-SNCA, and GCE-AuNPs-Ab1-BSA-SNCA-Ab2) were evaluated by CV, DPV, SWV, ChA techniques in 0.01 M $[Fe(CN)_6]^{3-/4-}$, which has been shown in Figure 1(A-F). According to obtained results, the characteristic peak of bare GCE was markedly increased from 23.02 µA to 49.98 µA and 12.76 µA to 23.41 µA in SWVs and DPVs, respectively. Also, the potential peak of bare GCE was decreased from 0.23 V to 0.19 V and 0.32 V to 0.26 V in SWVs, and CVs, respectively, after its modification with AuNPs. These evidences clearly demonstrated excellent characteristics of AuNPs in terms of specific surface area and conductivity enhancement. The presence of a highly conductive AuNPs layer on the GCE surface with a large surface area revealed the signal amplification for the redox probe, due to the improvement of the electron transfer process. Interestingly, conjugation of AuNPs with Ab1 definitely decreased the current intensity from 49.98 µA to 7.65 µA and 23.41 µA to 4.27 µA, which proved successful immobilization of antibodies on the GCE-AuNPs by covalent bond formation. Besides, the peak potential reduction for SWV, DPV and CV techniques from 0.19 V to 0.39 V, 0.2 V to 0.45 V and 0.26 V to 0.43 V as second evidence proved the immobilization of Ab1. Therefore, SNCA-Ab1, as a macromolecules assembly, blocked the electrode surface and decreased the efficiency of the electron exchange from the electroactive compound. In the next step, the current intensity was reduced again down to 3.83 µA and 2.79 µA due to blocking by BSA. After SNCA incubation, the current intensity has increased to 13.76 µA and 11.91 µA which indicates the formation of the Ab1-antigen-Ab2

complex. As it is obvious, formation of this immune complex reduces conductivity and limits electron transport. Also, the incubation of Ab2 for prepared GCE-AuNPs-Ab1-BSA-SNCA-Ab2 have led to increased CV peak current to 16.36 µA and reduced to peak current of DPV to 7.98 µA toward to hindered electron transfer effect.

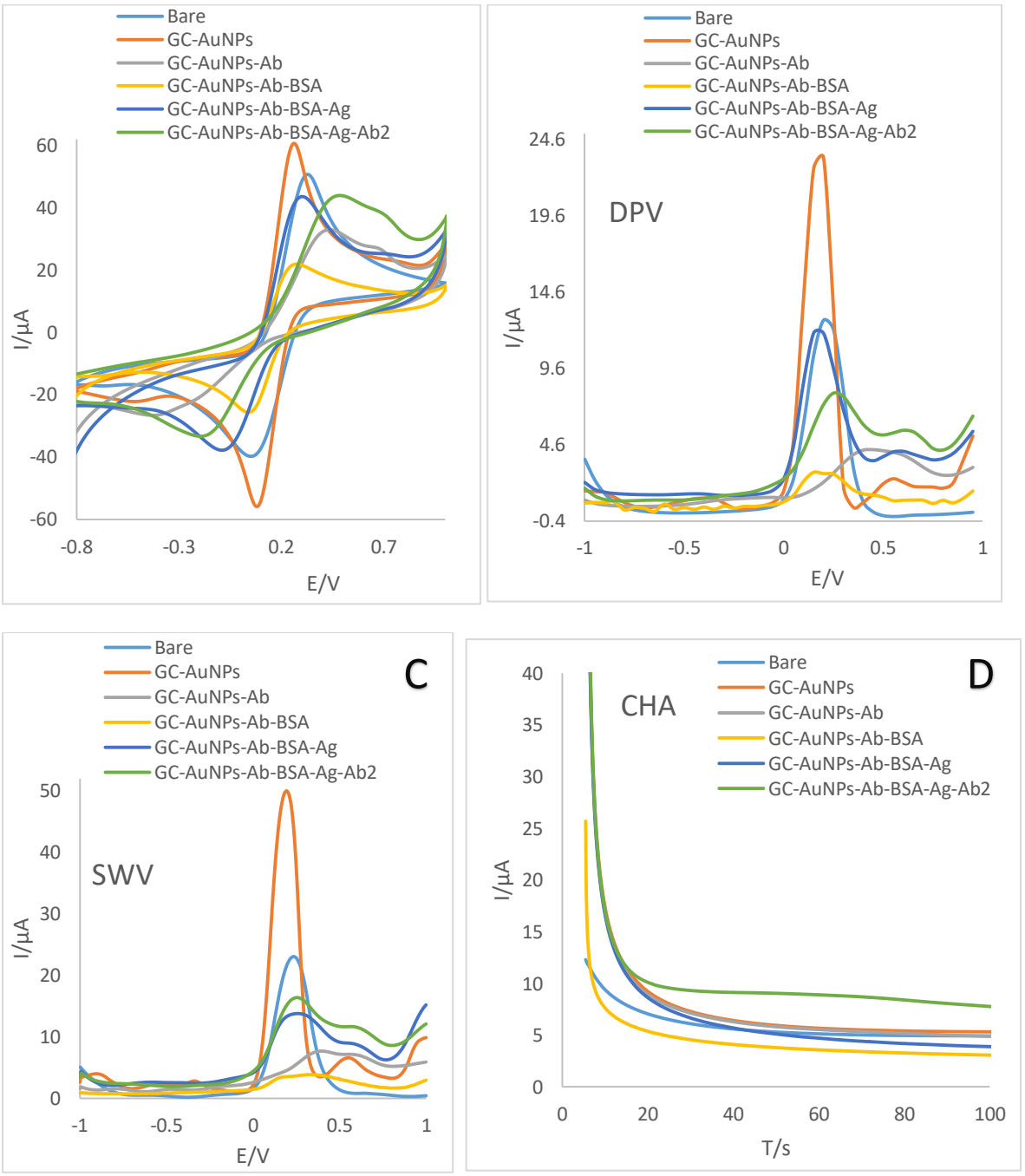

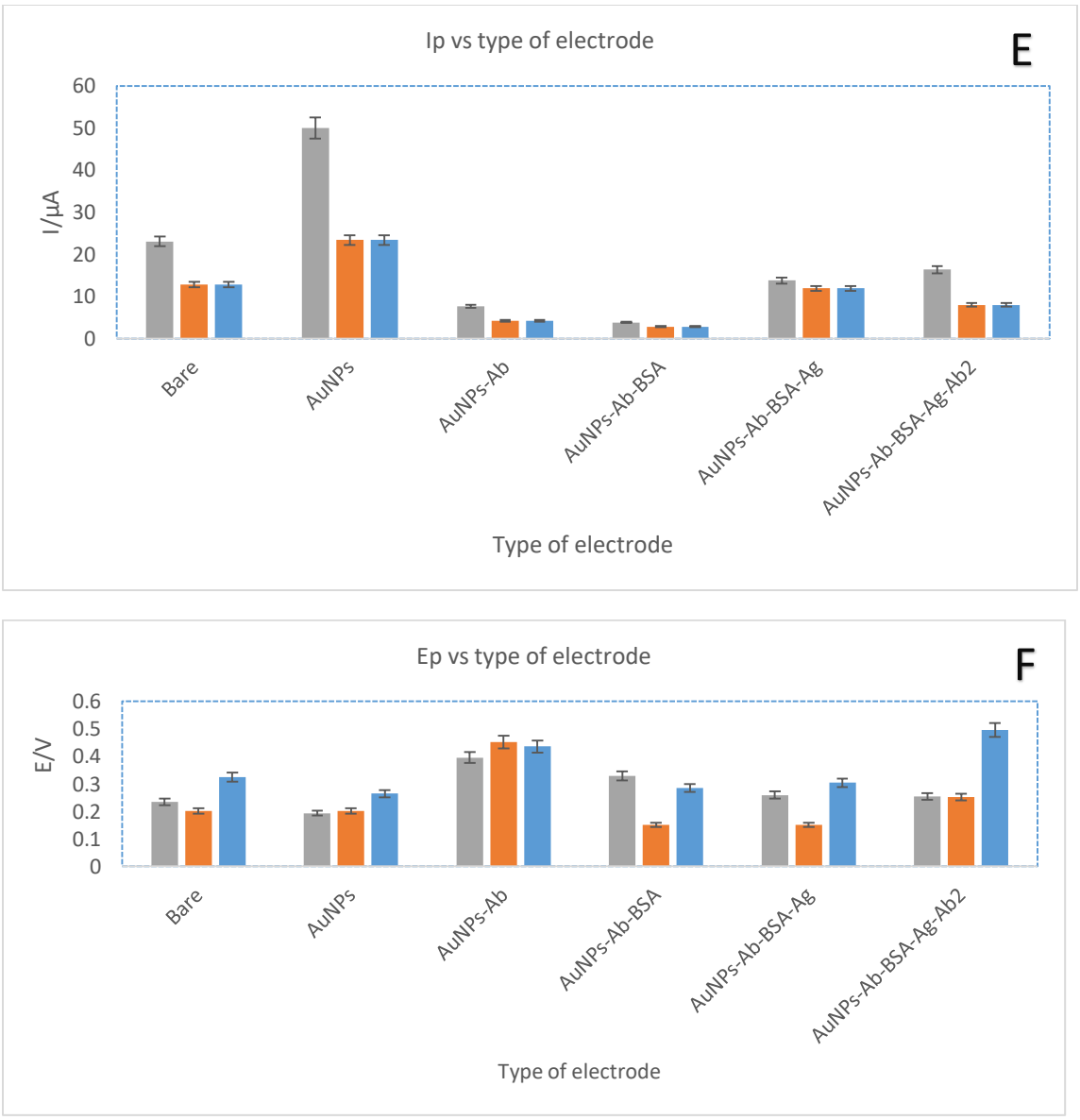

Figure 1. A) CVs, **B)** DPVs, **and C)** SWVs of GCE, GCE-AuNPs, GCE-AuNPs-Ab1, GCE-AuNPs-Ab1-BSA, GCE-AuNPs-Ab1-BSA-SNCA and GCE-AuNPs-Ab1-BSA-SNCA-Ab2 in a potential range of -1 to +1 V and scan rate of 100 mV/s in the solution of 0.01 $Fe(CN_6)^{3-/4-}$ and **D)** ChAs of modification surfaces in 0.01M $[Fe(CN)_6]^{3-/4-}$/KCl solution as electrochemical probe in E=0.3 V, duration time=100 s, **E)** Histogram of peak **current** *versus* type of electrode and **F)** Histogram of peak **potential** *versus* type of electrode.

Overall, electrochemical studies demonstrated that the fabricated immunosensor has high potential for capturing SNCA. It should be noted that the results of all four techniques have proven the results of each other.

3.3 Morphology of different modification of GCE-AuNPs

FE-SEM images of various steps of immunosensor fabrication GCE-AuNPs-Ab1, GCE-AuNPs-Ab1-BSA, GCE-AuNPs-Ab1-BSA-SNCA, and GCE-AuNPs-Ab1-BSA-SNCA-Ab2 are shown in Figure S4 A-F (see supporting information), respectively. Figure S4A-H (see supporting information) clearly demonstrated that antibodies were successfully immobilized on the surface of GCE-AuNPs. Also, success incubation of this bioreceptor revealed a guarantee for the effectiveness of the designing process. Furthermore, as you can see in Figure S5 A-K (see supporting information), BSA could efficiently block the unbinding functional groups on the AuNPs. The designed surface could capture the SNCA with high sensitivity and selectivity (Figure S6A-M (see supporting information)). Finally, Figure S7A-F (see supporting information) clearly demonstrated successful conjugation of Ab2 with the prepared surface (GCE-AuNPs-Ab1-BSA-SNCA). Besides, the EDX results (Figure S8 and 9 (see supporting information)) could provide complementary information to FE-SEM images. As you saw, the EDX results have proven the result of EDX.

3.4 Analytical performance

The specificity and sensitivity as a significant important part of developed immunosensor have evaluated by different concentrations of target analyte. For this purpose, the linear range and detection limit of fabricated biodevice was investigated by voltammetry and amperometry techniques in the presence of 0.01 M Ferricyanide/Ferrocyanide. In the presence of the different

concentrations of SNCA (0, 4, 8, 16, 32, 64 and 128 ng/ml), DPVs, SWVs and ChAs responses were recorded (Figure 2A-G).

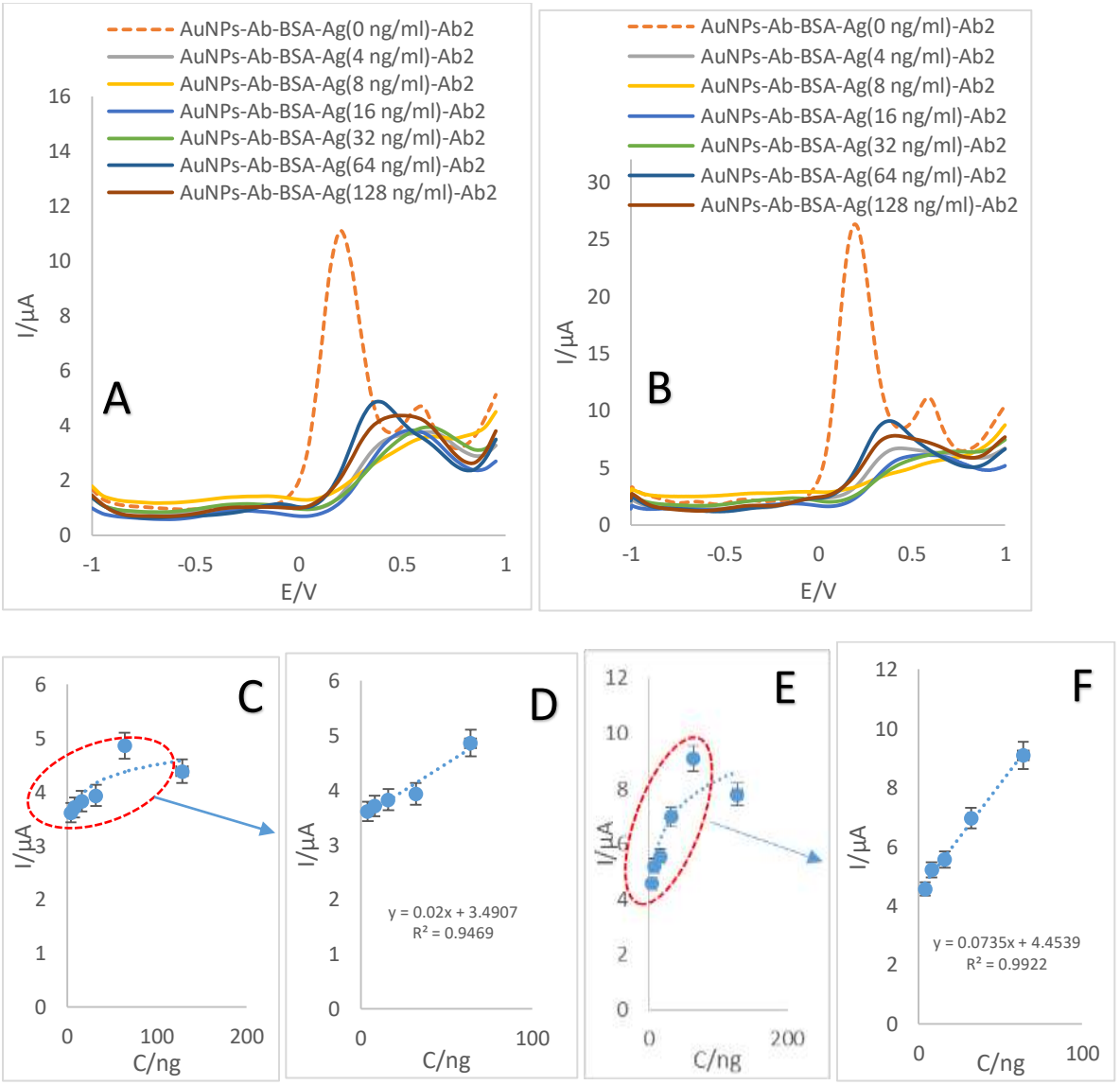

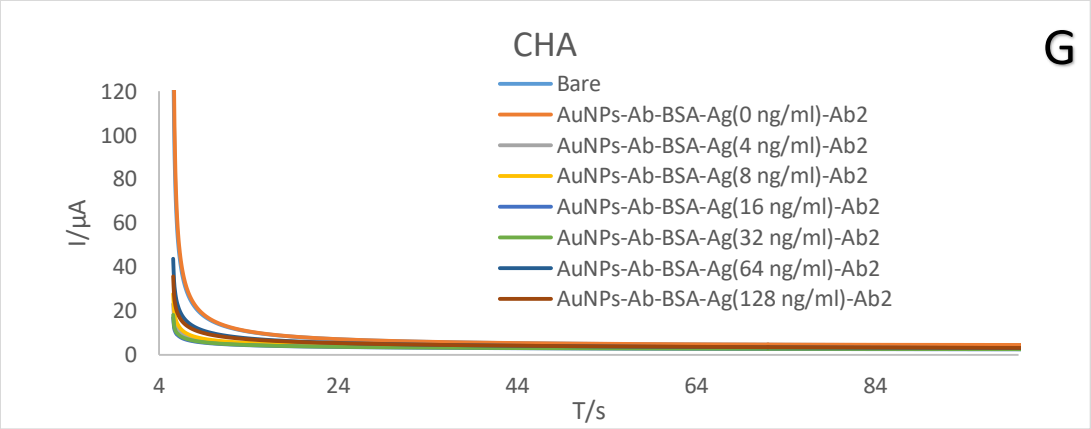

Figure 2. **A)** DPVs and **B)** SWVs of fabricated immunosensor for different concentrations of SNCA: (0, 4, 8, 16, 32, 64 and 128 ng/mL) in the presence of 0.01 M $[Fe(CN)_6]^{3-/4-}$ solution containing 0.1 M KCl. **C-F)** Calibration curves. **G)** ChAs of prepared immunosensor with different concentration of SNCA including 0, 4, 8, 16, 32, 64 and 128 ng/mL in the presence of 0.01 M $[Fe(CN)_6]^{3-/4-}$ solution containing 0.1 M KCl.

The calibration curve was achieved by drawing the peak current against the Neperian logarithm of SNCA concentration. According to obtained results, there is a linear relation between peak currents and antigen concentration which enhancing the concentration of SNCA caused increasing of peak current. The LLOQ and linear range of the designed immunosensor were 4 ng/ml and 4 to 64 ng/ml, respectively. The linear regressions equation achieved are as follows:

Linear regressions equation was obtained from dependency of peak current versus logarithm of concentration of SNCA using DPVs and SWVs is as:

$I\ (\mu A) = 0.02\ LogC_{(SNCA)} + 3.4907, \quad R^2 = 0.9469$
$I\ (\mu A) = 0.0735\ LogC_{(SNCA)} + 4.4539, \quad R^2 = 0.9922$

The ability of fabricated immunosensor for detection of low concentrations of target proved high potential of this biodevice for determination of SNCA. The analytical parameters of designed immunosensor were compared with other types of biosensors that developed for detection of

SNCA in Table 1 [33-36]. It can be conclude that the performance of the developed sandwich based immunosensor is comparable with or better than that of the currently developed approaches. In addition, most of the reported biosensors have operated on only one technique. However, our developed immunosensor exploited voltammetry and amperometry techniques. Subsequently, fabricated biodevice demonstrated great benefits including accuracy, biocompatibility and simplicity due to using low toxicity, high conductive and low-cost probe.

Table 1. A comparison of the performance of several assay strategies for determination of **α**-synuclein protein.

Assay strategies	Sensor Platform	Detection technique	Applied Sample	LOD/LOQ/LLOQ	Linear range	Ref
Immunosensor	Syn ab/PEG film /EDC-NHS/Au electrode	EIS[a]	Standard	21 ± 4 pM	0.05 to 2 nM	[33]
Immunosensor	Alpha-synuclein ab /EDC-NHS/PEG-thiol monolayer/Au electrode	EIS	Standard	55 ± 3 pM	0.5 to 10 nM	[34]
Aptasensor	aptamer/AuNPs	Colorimetric, SPR[b] and EIS	Standard	1 pM	-	[35]
Aptasensor	Apt-CS/SPGE[a]	Voltammetric	Standard	10 pM	60 pM to 150 nM	[36]
Immunosensor	GCE-AuNPs-ab-BSA-SNCA-Ab2	Voltammetry and amperometry	Standard and plasma	4 ng/ml	4 to 64 ng/ml	This work

a Electrochemical impedance spectroscopy

b Surface plasmon resonance

c screen-printed gold electrode

3.5 Real sample analysis

The application of developed immunosensor in complex biological fluids is always one of the most imperative factors, whether it is for practical application or for scientific researches. For this purpose, different antigen dilutions were mixed with plasma (4, 8, 16, 32, 64 and 128 ng/ml) (1:1 of plasma and antigen) and then it was dropped on the surface of the created biosensor. Afterwards, the DPV, SWV and ChA techniques were exploited for electrochemical signal measurement in 0.01 M of $[Fe(CN)_6]^{-3-/-4}$ and 0.1M KCl solution as the supporting electrolyte

(Figure S10A-C (see supporting information)) According to obtained results, the peak height and current intensity decrease with increasing the concentration of target. In the real sample, LLOQ and dynamic range of fabricated immunosensor were 4 ng/ml and 4 to 64 ng/ml, respectively.

3.6 Evaluation of specificity

The cross-reactivity is a common problem in immunosensors that result false-positive results, so the elucidation of specificity of immunosensor is a critical step in its development. For this means, a number of biomarkers interferers such as CA 15.3, CEA and PSA were used for specificity investigating of fabricated immunosensor. The CV, DPV, SWV and ChA technique in 0.01 M Ferricyanide/Ferrocyanide results showed that peak potential of SNCA was more than other interfere agents. For instance, the location of peak potential for PSA, CEA, CA 15.3 and SNCA were 0.2, 0.59, 0.54 and 0.7 V, respectively in CVs (Figure 3 (A-F)). Additionally, the peak current of other interfering agents were more than SNCA (the peak intensity of PSA, CA 15.3, CEA, and SNCA in SWVs, DPVs and CVs were 48.37, 43.18, 42.96 and 31.15 µA and 5.58, 5.18, 4.3 and 3.7 µA and 12.87, 8.37, 7.08 and 6.29 µA, respectively). Therefore, the results of all techniques demonstrated that our designed immunosensor has good specificity in detecting SNCA.

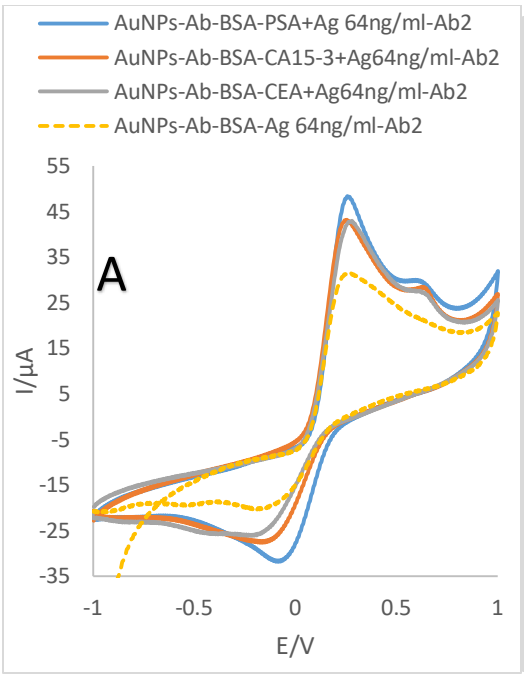

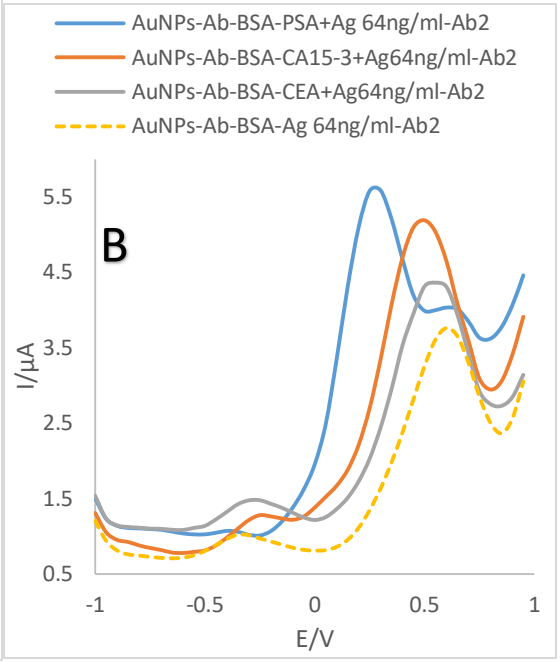

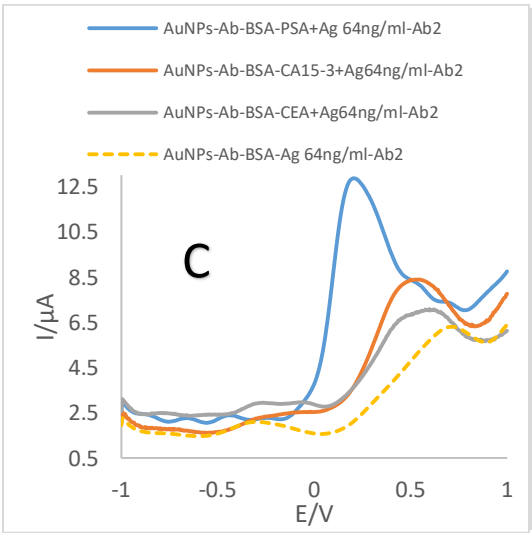

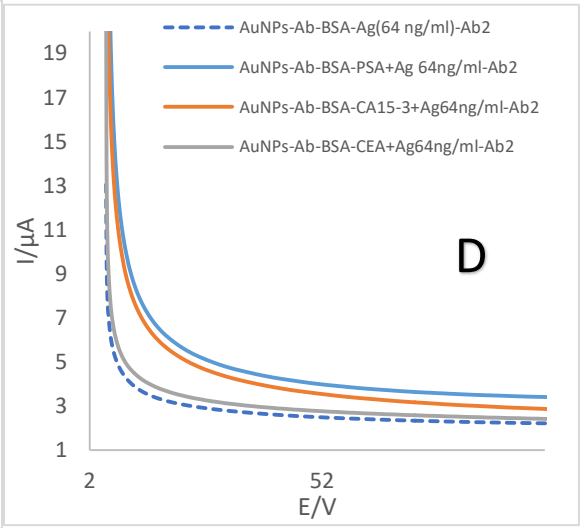

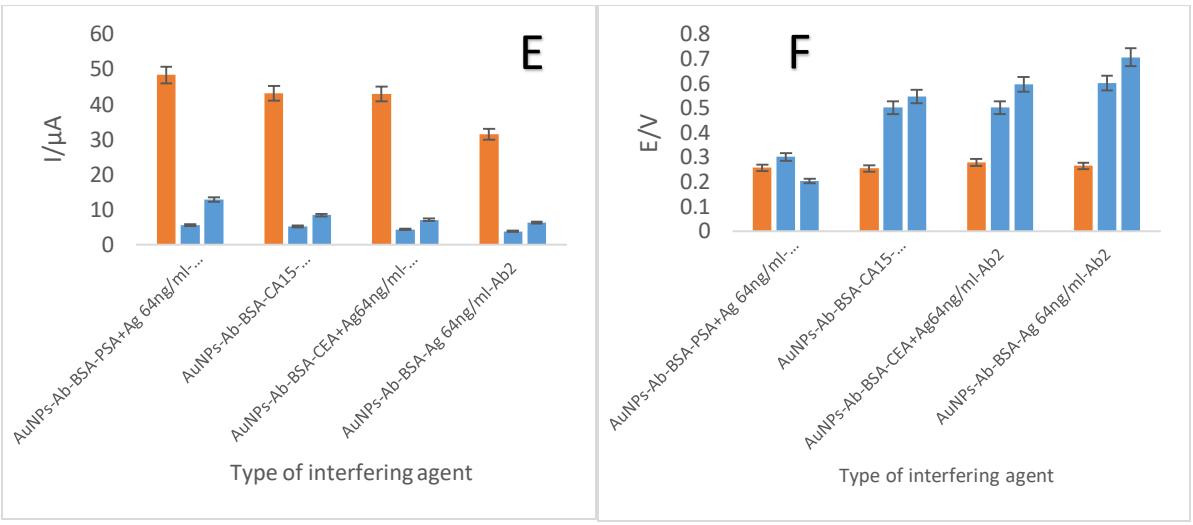

Figure 3. A) CVs, **B)** DPVs, **and C)** SWVs and **D)** ChA of the designed immunosensor in the presence of SNCA, (CA 15.3+SNCA), (CEA+SNCA), and (PSA+ SNCA) in 0.01M $[Fe(CN)_6]^{3-/4-}$/KCl solution as supporting electrolyte. **E-F)** Histograms of peak current and potential versus type of interfering species, respectively.

3.7. Stability and repeatability of the fabricated immunosensor

Intra-day and inter-day tests as critical issues for the commercial application have investigated by CV technique for measuring reproducibility of developed immunosensor. In details, inter-day stability of immunosensor has been established in 0.01 M $[Fe(CN)_6]^{3-/4-}$ along with 0.1 MKCl solution 4 times (every 2h) within a day in similar conditions and interval times. The peak currents for both oxidation and reduction peaks decrease 42% until 4 h (Figure S11 G-H (see supporting information)). However, the performance of the immunosensor was changed after 6h (Figure S11 A-B (see supporting information)). Moreover, inter-day precision of biodevice has been carried out over four days and the highest current peak was measured on the first day (Figure S11 C-D (see supporting information)). The investigations of cyclic stability of immunosensor in 0.01 M Ferricyanide/Ferrocyanide by CV technique demonstrated that the current of peak was decreased step-by-step (Figure S11E-F (see supporting information)). The

reproducibility of the fabricated immunosensor was measured by recording the current intensity of five separate electrodes. According to the obtained results, the developed immunosensor has relatively low reproducibility (Figure S11 (I-K) (see supporting information)) which is negative part of this research study. It worth to noted that during this period, the electrodes were kept at 4 °C.

3.8. Kinetic study

The study of scan rates on electrochemical system under study exhibits important information about electrochemical mechanisms of electron transfer, which can acquire from the relationship between the peak current/potential and sweep rate. The effect of scan rate on the electrochemical behavior of GCE-AuNPs was investigated in in the range of 10-1000 mV/s in an electrochemical cell containing 0.01 M $[Fe(CN)_6]^{3-/4-}$. As shown in Figure S12A (see supporting information), increasing of the scan rate led to increase in peak currents and the oxidation peak potentials were shifted to positive range. The acquired related plots were demonstrated in Figure S12 (see supporting information). The relation between peak current and potential sweep rate can be described by Eq. 1 [37]:

$$Ip = \left(\frac{n^2F^2}{4RT}\right)\nu A\Gamma^* \qquad (1)$$

In this equation, ν is the potential sweep rate and A is the electrode surface area ($A=\pi r^2$). Γ^* has been obtained as 0.43670 $mol.cm^{-2}$ by equation (1). In addition, the peak currents versus square root of different sweep rates indicated in Figure S12C (see supporting information), which shows a linear relation, indicating diffusion controlled mass transfer of oxidation process on electrode surface. According to the obtained result, electrochemical process was controlled by diffusion of species (Figure S12B (see supporting information). Another reason for proving the mass transfer was controlled by diffusion was Figure S12F (see supporting information). As you can see, the

slope of the chart is close to 50. The value of the electron-transfer coefficient was computed by the equation 2 [38]:

$$E = \left(\frac{RT}{2\alpha F}\right) lnv + constant \qquad (2)$$

Thus, this value was calculated to be around 0.3193, which prove the irreversible nature of the electrode diffusion process.

4. Conclusion

To sum up, a novel, sandwich type electrochemical immunosensor was developed for sensitive and specific quantification of SNCA protein. For this purpose, a durable AuNPs layer was successfully prepared by electrodeposition onto the GCE surface. The AuNPs with large number of active functional groups provide enhanced electrical conductivity and extensive surface area. Also, they offer a satisfactory loading sites for antibodies to specific determination of SNCA. Therefore, this metallic based substrate can improve the electrochemical active surface to interact with SNCA. Under the optimized operating conditions, the fabricated immunosensor demonstrated acceptable linear range 4 to 64 ng/ml and LLOQ of 4 ng/ml for determination of SNCA in standard buffer and real samples. It is expected that the proposed immunosensor can be utilized as a versatile system for other biomarkers quantification especially in clinical diagnostics owing to good performance and high sensitivity.

Declaration of Competing Interest

The authors declare that they have no known competing financial interests or personal relationships that could have appeared to influence the work reported in this paper.

Acknowledgment

The authors would like to thank the Tabriz University and Tabriz University of Medical Sciences.

CRediT authorship contribution statement

Esmaeil Darvish Aminabad; Experimental works, Writing - original draft.
Mohammad Hasanzadeh; Conceptualization, writing-original draft, review & editing
Ali Ahmad Alipour; Conceptualization, review & editing
Tohid Mahmoudi; review & editing
Mohammad Ali Hosseinpour Feizi; Conceptualization, Review & editing.
Reza Safaralizadeh; Review & editing
Ahmad Mobed; Experimental works, Writing - original draft.

References

1. A. Schapira, Parkinson's disease, *Bmj* 318(7179) (1999) 311-314.

2. M. Politis, K. Wu, S. Molloy, P. G. Bain, K.R. Chaudhuri, P. Piccini, Parkinson's disease symptoms: the patient's perspective, *Movement Disorders* 25(11) (2010) 1646-1651.

3. S. Sveinbjornsdottir, The clinical symptoms of Parkinson's disease, *Journal of Neurochemistry* 139 (2016) 318-324.

4. R.L. Nussbaum, C.E. Ellis, Alzheimer's disease and Parkinson's disease, *New england journal of medicine* 348(14) (2003) 1356-1364.

5. D. Calne, J.W. Langston, Aetiology of Parkinson's disease, *The Lancet* 322(8365-8366) (1983) 1457-1459.

6. W. Dauer, S. Przedborski, *Neuron* 39(6) (2003) 889-909.

7. C.R. Freed, P.E. Greene, R.E. Breeze, W.-Y. Tsai, W. DuMouchel, R. Kao, S. Dillon, H. Winfield, S. Culver, J.Q. Trojanowski, *New England Journal of Medicine* 344(10) (2001) 710-719.

8. J. Segura-Aguilar, I. Paris, P. Muñoz, E. Ferrari, L. Zecca, F.A. Zucca, Protective and toxic roles of dopamine in Parkinson's disease, *Journal of Neurochemistry* 129(6) (2014) 898-915.

9. N. Ball, W.-P. Teo, S. Chandra, J. Chapman, *Frontiers in neurology* 10 (2019) 218.

10. P. Jenner, *Annals of Neurology: Official Journal of the American Neurological Association and the Child Neurology Society* 53(S3) (2003) S26-S38.

11. L. Stefanis, Cold Spring Harbor perspectives in medicine 2(2) (2012) a009399.

[12. A. Recchia, P. Debetto, A. Negro, D. Guidolin, S.D. Skaper, P. Giusti, *The FASEB Journal* 18(6) (2004) 617-626.

13. M.S. Goldberg, P.T. Lansbury Jr, *Nature cell biology* 2(7) (2000) E115-E119.

14. V. Ghiglieri, V. Calabrese, P. Calabresi, *Frontiers in neurology* 9 (2018) 295.

15. C.R. Fields, N. Bengoa-Vergniory, R. Wade-Martins, *Frontiers in molecular neuroscience* 12 (2019) 299.

16. E. Maries, B. Dass, T.J. Collier, J.H. Kordower, K. Steece-Collier, TN*ature Reviews Neuroscience* 4(9) (2003) 727-738.

17. A.L. Biere, S.J. Wood, J. Wypych, S. Steavenson, Y. Jiang, D. Anafi, F.W. Jacobsen, M.A. Jarosinski, G.-M. Wu, J.-C. Louis, *Journal of Biological Chemistry* 275(44) (2000) 34574-34579.

18. L.L. Venda, S.J. Cragg, V.L. Buchman, R. Wade-Martins, *Trends in neurosciences* 33(12) (2010) 559-568.

19. B. Mollenhauer, V. Cullen, I. Kahn, B. Krastins, T.F. Outeiro, I. Pepivani, J. Ng, W. Schulz-Schaeffer, H.A. Kretzschmar, P.J. McLean, *Experimental neurology* 213(2) (2008) 315-325.

20. S.J. Lincoln, O.A. Ross, N.M. Milkovic, D.W. Dickson, A. Rajput, C.A. Robinson, S. Papapetropoulos, D.C. Mash, M.J. Farrer, *Parkinsonism & related disorders* 13(6) (2007) 340-342.

21. J. Fuchs, A. Tichopad, Y. Golub, M. Munz, K.J. Schweitzer, B. Wolf, D. Berg, J.C. Mueller, T. Gasser, G *The FASEB journal* 22(5) (2008) 1327-1334.

22. Q. Hassan, S. Li, C. Ferrag, K. Kerman, *Analytica chimica acta* 1089 (2019) 32-39.

23. H.K. Kordasht, M. Hasanzadeh, *Analytical Methods* 12(22) (2020) 2795-2811.

24. Y. Huang, J. Xu, J. Liu, X. Wang, B. Chen, *Sensors* 17(10) (2017) 2375.

25. A. Muir, R. Porteous, R. Wastie, *Journal of Agricultural Engineering Research* 27(2) (1982) 131-138.

26. K. Wong-Ek, O. Chailapakul, J. Prommas, K. Jaruwongrungsee, N. Nuntawong, A. Tuantranont, QCM based on flow system for cardiovascular disease, World Congress on Medical Physics and Biomedical Engineering, September 7-12, 2009, Munich, Germany, Springer, 2009, pp. 80-83.

27. H. Karimi-Maleh, F. Karimi, L. Fu, AL. Sanati, M. Alizadeh, C Karaman, Y. Orooji. *J. Haz Mater* 423 (2021) 127058.

28. H. Karimi-Maleh, M. Alizadeh, F. Karimi, M. Baghayeri, L. Fu, J. Rouhi, C. Karaman, R. Boukherroubk. *Chemosphere*, 2021, 132928, doi.org/10.1016/j.chemosphere.2021.132928..

29. F. Ricci, G. Adornetto, G. Palleschi, *Electrochimica Acta* 84 (2012) 74-83.

30. H. Karimi-Maleh, M. Alizadeh, Y. Orooji, F. Karimi, M. Baghayeri, J. Rouhi, S. Tajik, Hadi Beitollahi, S. Agarwal, V.K. Gupta, S. Rajendran, S. Rostamnia, L. Fu, F. Saberi-Movahed, S. Malekmohammadi. *Ind Engin Chem Res* 60 (2), 2021, 816-823.

31. SAR Alavi-Tabari, MA Khalilzadeh, H Karimi-Maleh. *J. Electroanal Chem* 811, 2018, 84-88.

32. H Karimi-Maleh, F Tahernejad-Javazmi, AA Ensafi, R Moradi, H. Beitollahi. Biosens Bioelectron 60, 2014, 1-7.

33. Q. Xu, S. Evetts, M. Hu, K. Talbot, R. Wade-Martins, J.J. Davis, *RSC Advances* 4(102) (2014) 58773-58777.

34. T. Bryan, X. Luo, L. Forsgren, L.A. Morozova-Roche, J.J. Davis, T *Chemical Science* 3(12) (2012) 3468-3473.

35. K. Sun, N. Xia, L. Zhao, K. Liu, W. Hou, L. Liu, *Sensors and Actuators B: Chemical* 245 (2017) 87-94.

36. S.M. Taghdisi, N.M. Danesh, M.A. Nameghi, M. Ramezani, M. Alibolandi, M. Hassanzadeh-Khayat, A.S. Emrani, K. Abnous, *Biosensors and Bioelectronics* 123 (2019) 14-18.

37. A.L. Eckermann. *Coordination Chem. Reviews*, 254 (2010) 1769-1802.

38. RS. Nicholson, I. Shain, *Anal. Chem*, 1964, **36**, 706-723.